

STUDY OF A WASTE HEAT RECOVERY ORGANIC RANKINE CYCLE FROM A SULFURIC ACID PRODUCTION PLANT

Nawel BEN ALI¹, Aicha MABROUK², Nejib HAJJI³

^{1,2}University of Gabes, National engineering school, Department of Chemical Engineering, Omar Ibn-Elkhattab street, 6072 Gabes, Tunisia.

Email: benalinawel16@gmail.com;

ABSTRACT

In this paper, the study of electrical energy production by Organic Rankine Cycle (ORC's) was considered for the valorization of waste heat stemming from a sulfuric acid production plant. First, a sensitivity analysis was carried out to study the effect of different operating parameters on the thermal efficiency of the cycle. These parameters include the evaporation pressure, the evaporation temperature, the condensation temperature, the cooling water temperature as well as the efficiency of the turbine and the pump. Energy calculations were obtained from the process simulation with Aspen HYSYS. A total of 24 potential working fluids were considered in this study with emphasis on ammonia. The selection among them was based not only on thermal efficiency but also on environmental and safety considerations. Benzene and ammonia were found to be the most efficient. Results proved that it is possible to produce 7 MW of electricity in the considered plant using ORC's.

Keywords: Organic Rankine cycle, sensitivity analysis, thermal efficiency, HYSYS, working fluid.

1. INTRODUCTION

Energy reserves are diminishing and the excessive use of fossil fuels is causing serious environmental problems. Hence, it is necessary to rely on cleaner sources of energy like the renewable energy and the recovery of industrial waste heat which are gaining increasing worldwide interest.

Therefore, a significant amount of energy is often wasted in the form of thermal releases that are generated as a by-product and released directly into the environment. Actually, 20 to 50% [1-3] of energy consumption in the industrial sector is dissipated as waste heat has a low to medium temperature. Indeed, nearly 90% of industrial heat discharges have a temperature not exceeding 316°C about 60% of which have a temperature below 230°C [4].

Currently, recovering and converting low temperature heat waste into electricity is of great interest. This not only improves the energy efficiency of industrial processes, but also reduces the thermal pollution caused by the direct discharge of heat into the environment. The organic Rankine cycles (ORC's) is one of the promising technologies were developed for this purpose. Since the 1970's, many theoretical and experimental studies of ORC technology have been reported for various sources of energy including waste heat recovery [5-7], solar [8-10] and geothermal energy [11-14]. ORC has been introduced as an alternative to the conventional steam Rankine cycle to be used as a bottoming cycle for combined power plants. Several working fluids are used in this cycle, such as hydrocarbons, refrigerants and siloxane [15]. These fluids are more adapted than water for the recovery of heat from low temperature sources due to their low boiling points [16]. In all studies, a satisfactory thermodynamic performance was achieved using ORC cycles. However, their thermal efficiency still needs to be improved.

The choice of the working fluid is one of the main factors affecting the operation of the cycle. Therefore, several authors studied the selection of suitable working fluids for energy recovery [17-18]. This selection depends on the source of energy application and the level of heat to be used. The fluid of choice must yield a high efficiency and show good thermodynamic properties. Stability, environmental impact, toxicity, safety, compatibility, availability and cost are also important in the selection process.

Su et al. [18] developed a model for the choice of working fluids and the optimization of cycle parameters at the molecular scale. Based on their criteria, R254eb and R254cb were found to be the optimal fluids.

Wang et al. [5] considered 13 fluids and found that R123 is the most suitable when the temperature of the hot source is between 100 and 180°C and that R141b is the best for higher temperatures. They also found that the cycle is no longer economical when the temperature of the source is below 100°C. Saleh et al. [17] compared the thermodynamic performances of 31 pure working fluids for different types of ORC using the BACKONE equation of state. They found that the highest efficiency is obtained for high boiling substances. E. Ozah et al. [19] studied the use of an exhaust gas at 566°C as an energy source based on four working fluids, namely toluene, octamethyltrisiloxane (MDM), octamethylcyclotetrasiloxane (D4) and n-decane. The optimization of the cycle was performed using the genetic algorithm method (NSGA-II) written in MATLAB.

Thurairaja et al. [20] analyzed the properties of ozone-friendly low-boiling working fluids for ORC using the “REFPROP” database. They found that MD2M and cyclopentane for temperature ranges 50 - 100 °C, butane, neopentane and R245fa for 100 - 150 °C, ethanol, methanol and propanone for 150-200°C and Water, m-Xylene and p-Xylene for 200 - 320 °C are better working fluids for energy extraction. S.Quoilin et al. [21] investigated the thermo-economic optimization of an ORC cycle using waste heat based on 5 fluids. They found that n-butane is the most economical option. Furthermore, the optimal thermodynamic value is also given by n-butane with an overall efficiency of 5.22%. Vivian et al. [22] studied the selection of working fluids and the performance of cycle configurations for a given heat source using four different ORC configurations and 27 working fluids based on cycle efficiency and heat source recovery factor. Hærvig et al. [23] developed guidelines on how to choose the optimal working fluids based on the hot source temperature investigating 26 commonly used working fluids based on the net power for hot source temperatures ranging from 50 to 280°C.

Recent studies include the use of zeotropic mixtures [24]. A comprehensive review of ORC working fluids is presented by Bao and Zhao [25]. They compared 77 common pure components and 44 zeotropic blends. Other researchers focused on different parameters for improving the cycle efficiency like temperature and pressure at the inlet of the turbine [26-28].

Hence, one of the most pertinent challenges in ORC is the selection of the working fluid. This selection should be accompanied by a parametric optimization of the cycle because the operating conditions have a strong effect on its performance.

The present work is aimed at studying the production of electrical energy by Organic Rankine Cycle through the use of waste heat coming from an existing sulfuric acid production unit. The waste heat was estimated at 23 MW for a production of 1500 tons of sulfuric acid per day. Up to 9 MW of this waste can be recovered as hot water at 110°C [29] and used to operate an ORC.

In order to study this operation, a simulation was performed using Aspen Hysys. Then, a sensitivity analysis was conducted in order to assess the effect of different parameters on the cycle performance. The choice of the study of these parameters was performed based on earlier studies [5], [30-31]. These parameters are the temperature at the inlet of the turbine, the temperature at the outlet of the condenser, the pinch point in the generator and the condenser as well as the high and low pressures. Simulations were conducted for various working fluids but the emphasis was placed on ammonia because it is stored in significant amounts in the same chemical plant. The obtained results were compared to those given by Engineering Equations Solver (EES) software.

2. METHODOLOGY AND THEORETICAL BACKGROUND

2.1. SYSTEM DESCRIPTION

The global system (fig.1) consists of a hot water loop shown in red connected to the ORC cycle which shown in blue. It is composed mainly of six pieces of equipment which are the acid-water heat exchanger, the turbine, the generator, the condenser and tow pumps. The working fluid passes through four thermodynamic states. It evaporates at high pressure in the evaporator using heat provided by the water circulating in the hot water loop (state 1) and then expands in the turbine (state 2) which drives an alternator for the production of electricity. Afterwards, it condenses in the condenser at the low pressure (state 3) and finally passes through the pump (state 4) which returns it to the generator. Using this system, the heat given by the sulfuric acid drives the cycle instead of being rejected to the environment.

2.2. FLUID SELECTION

The selection of a suitable working fluid for the Rankine cycle is difficult because of the availability of a great number of potentially suitable substances for each range of temperature and also because of the variation of the cycle working conditions for each fluid [25]. Therefore, the selection of working fluids has been treated in a large number of scientific publications [17, 19, 20]. In most cases, these studies compare between a set of candidate fluids based mainly on thermodynamic performances and total costs. The most important criteria which are usually considered for the selection are: the slope of the saturated vapor curve in the temperature-entropy diagram, vapor density, viscosity, fluid freezing point, temperature stability, safety level, conductivity, evaporation pressure, fluid condensation pressure, Ozone Depletion Potential (ODP), Greenhouse Warming Potential (GWP) [30][32-35].

Based on these criteria, 24 fluids that can be used for ORC systems are chosen to study their effect on the energetic performance of the cycle. Table 1 summarizes the properties of these fluids. This table indicates that, despite the extensive work conducted on this subject, no single fluid has been identified as optimal for these systems. For instance, some authors consider the environmental impact (ODP, GWP), the flammability and the toxicity of the working fluid, while others do not. All these properties are necessary to evaluate the effect of the working fluid on the environment as well as the size and cost of the cycle.

2.3. ORC CYCLE MODELING

2.3.1. Assumptions

The following assumptions are made throughout this study:

- The cycle operates at steady state,
- The condensate leaves the condenser as a saturated liquid,
- Pressure drop and heat losses in the pipes are neglected,
- The available power extracted from the hot water loop is equal to 9 MW [29], 2.3.2.

Energy analysis

Aspen-HYSYS was used to simulate the ORC and the thermodynamic properties of the working fluids were estimated using the Peng-Robinson Equation of State [39].

The thermal efficiency of the cycle was taken as the performance indicator. Its value is calculated using equation 1 [35]:

$$\eta_{th} = \frac{\dot{W}_{net}}{\dot{Q}_{gen}} = \frac{W_t - W_p}{\dot{Q}_{gen}} \quad (1)$$

The mass flow rate of the working fluid is given by equation 2 [40]:

$$\dot{m}_f = \frac{\dot{Q}_{gen}}{h_{inlet,hotwater} - h_{outlet,hotwater}} \quad (2)$$

The power given by the turbine (W_t) and that consumed by the pump (W_p) are determined using equations 3 and 4, respectively [40]:

$$W_t = \dot{m}_f (h_1 - h_2) \quad (3)$$

$$W_p = \dot{m}_f (h_4 - h_3) \quad (4)$$

An isentropic efficiency is used for the turbine to describe the irreversible expansion process [41]:

$$\eta_t = \frac{h_2 - h_1}{h_2 - h_{1,is}} \quad (5)$$

The isentropic efficiency of the pump is given by equation 6 [41]:

$$\eta_p = \frac{h_{4,is} - h_3}{h_4 - h_3} \quad (6)$$

For the generator, the heat duty is determined by [40]:

$$\dot{Q}_{gen} = \dot{m}_f (h_1 - h_4) \quad (7)$$

The heat duty of the condenser is given by [41]:

$$\dot{Q}_{cond} = \dot{m}_f (h_3 - h_2) \quad (8)$$

It should be noted that these equations are necessary only for EES as Hysys contains its own model library.

3. RESULTS AND DISCUSSION

3.1. Sensitivity analysis

In this section, a sensitivity analysis is conducted in order to reveal the influence of the decision parameters on the cycle performance. These parameters are: condensation temperature, condensation pressure, evaporation temperature, evaporation pressure, pinch point in condenser and generator as well as the isentropic efficiency of turbine and pump. Table 2 gives the values of the operating parameters.

3.1.1. Effect of the condensation temperature and pressure

As can be seen in fig. 2, the condensation temperature (T_3) has an influence on the thermal efficiency. Indeed, the lower the value of this temperature, the higher the efficiency is. Furthermore, this temperature is related to that of the cooling water at the inlet of the condenser and its value must be greater. The difference between them is the pinch point in the condenser. Subsequently, the lower the cooling water temperature and the smaller the pinch point, the lower T_3 and the higher the efficiency. Hence, the pinch point was taken equal to 5°C in this work [40].

Since the working fluid is a saturated liquid at the outlet of the condenser, its temperature is directly related to its pressure. Consequently, as shown in fig. 3, by decreasing the condensation pressure, the cycle efficiency becomes greater due to the decrease in the condensation temperature.

3.1.2. Effect of the evaporation temperature and the pinch point in the generator

As shown in fig.4, the efficiency of the cycle increases with the evaporation temperature. As a result, it

increases with the decrease of the pinch point in the generator which is also chosen small and equal to 10°C [41] to assure an evaporation temperature of 100°C.

3.1.3. Effect of the evaporation pressure

The evaporation pressure also has an important effect on the thermal efficiency (fig.5). Increasing the evaporation pressure on the one hand increases the thermal efficiency, but on the other hand, decreases the vapor fraction at the outlet of the turbine that must exceed 0.9 to prevent damage to its blades. Hence, the evaporation pressure should be set as high as possible to maximize the thermal efficiency, but without allowing the vapor fraction at the outlet of the turbine to go below 0.9. According to Badr et al. [42], the appropriate pressure range for the ORC operation is between 0.1 and 2.5 MPa. Among the 24 fluids considered in this study, only benzene, toluene, cyclohexane, n-octane and n-heptane have an optimum evaporation pressure.

3.1.4. Effect of the isentropic efficiencies of the turbine and the pump

The effect of the isentropic efficiencies of the turbine and the pump are presented in fig.6 and fig.7, respectively. Note that, unlike the pump, the efficiency of the turbine has a great effect on the cycle performance. In this work, the isentropic efficiency of the turbine is set at 90% and the isentropic efficiency of the pump at 80% according to the literatures [43] and [44], respectively.

3.2. Comparison between the studied working fluids

Based on the sensitivity analysis, the parameters that have a greater effect on the cycle performance were found to be the condensation temperature, the evaporation temperature and the evaporation pressure. The evaporation temperature is set at 100 °C because it is limited by the source of energy. The value of the optimum evaporation pressure depends on the working fluid. Fig.8 shows the effect of the evaporation pressure on the thermal efficiency of the cycle for the different fluids presented in Table 1 for a condensation temperature of 28°C. It shows that the optimum pressure is not the same for all fluids. The condensation temperature depends on the temperature of the cold fluid which corresponds to the ambient temperature. To further compare between the 24 studied fluids, the energy performance of the various fluids is calculated in the case of three different values of the condensation temperature: 28 ° C, 40 ° C and 50 ° C. In each fixed value of this temperature, the optimum evaporation pressure is determined for each working fluid.

Table 3 gives the maximum thermal efficiency for each fluid as well as the mass flow rate, the produced power and the evaporation pressure that go with it for the same condensation temperature. The working fluids are sorted according to the thermal efficiency they yield for the cycle. Tables 4 and 5 illustrate the same results for condensation temperatures of 40 and 50°C, respectively.

Each working fluid has a specific evaporation pressure range. The lower bound of this interval must be larger than the saturation pressure at the condensation temperature. The upper limit is chosen that the vapor fraction at the outlet of the turbine does not go below 0.9. Only 6 fluids have an optimum evaporation pressure corresponding to a vapor fraction at the outlet of the turbine which is less than 1. These are: cyclopropane, R152a, NH₃, R134a, R290, R1270 and R143a.

Tables 3 to 5 show that the thermal efficiency is greatly affected by the condensation temperature which is directly related to the ambient temperature. They also show that the condensation temperature affects the mass flow rate required for producing a given power from a fixed heat duty in the generator.

The produced power is proportional to the thermal efficiency since the heat duty given by the water loop is constant (9 MW). Since the maximum yield obtained in this study is about 15.4%, a maximum power of 1.4 MW can be produced by the ORC and this can be reached only when benzene is used as a working fluid. Given that the chemical plant contains five sulfuric units of the same production capacity, a maximum of 7 MW can be obtained using this technology.

4. MATHEMATICAL MODEL VALIDATION

For the sake of comparison, the results given by HYSYS were checked with EES for all studied fluids except cyclopentane, cis-butene, transbutene and cyclopropane because they are not found in the EES library composition. According to tables 6 to 8, the results given by the two software tools were in good agreement for all the considered condensation temperatures. Therefore, the relative difference in results given by the two software tools is very small (less than 5%) for all the tested fluids.

In order to further validate the obtained results, the developed simulation model is compared with the results presented in the study of Wang et al [31] for the working fluid R141b. The comparison is based on the same input parameters values used in literature [31] which are summarized in Table 9. The comparison shows very good agreement between the present solution and the results of Wang et al, as indicated in Table 10. Hence, it can be concluded that the numerical calculation of the thermodynamic modeling of the systems is reliable.

5. CONCLUSION

Electricity production using waste heat from a sulfuric acid production plant was studied in this work. To this end, an Organic Rankine Cycle was simulated using Hysys for various potential working fluids and different operating conditions.

The obtained results showed that, besides availability, the use of ammonia as working fluid for this application can be justified by the circulation rate. However, the highest efficiency was given by benzene.

Hence, two scenarios can be considered for the operation of the ORC which are:

- The use of ammonia as working fluid. In this case, and based on the efficiency obtained for this fluid and the heat that can be extracted from the hot water loop, 1.2MW of electricity can be generated by the ORC per unit. It should be mentioned that the use of ammonia will be of no difficulty to the technicians because they are already working with it in the plant.
- The use of benzene as working fluid. In this case, up to 1.4 MW of electricity can be generated per unit but special precautions will be needed due to the health hazards associated with this fluid.

Finally, since the industrial plant contains five sulfuric acid production units of the same capacity, a total of 7MW of electricity can be generated from heat waste using this technology.

Nomenclature

| | |
|-----------|--------------------------|
| h | Specificenthalpy, kJ/kg |
| \dot{m} | Masse flow rate, kg/s |
| T | Temperature, °C |
| ORC | Organic Rankine cycle |
| P | Pressure, kPa |
| Q | Heat transfer rate, kW |
| w | Power, kJ/kg |
| s | Specificentropy, kJ/kg.K |
| | Power, kW |
| \dot{W} | |
| x | Vapor fraction |

Greek symbol

| | |
|--------|-----------------------------|
| η | Efficiency, % |
| ρ | Density, kg·m ⁻³ |

subscript

| | |
|---------|---------------------|
| am | Ambient |
| 1,2,3,4 | State 1, 2, 3 and 4 |
| b | Boiling |
| c | Critic |
| cond | Condenser |
| ev | Evaporation |
| fl | Fluid |

| | |
|-----|------------|
| Gen | Generator |
| is | Isentropic |
| in | Inlet |
| max | Maximum |
| net | Net |
| out | Outlet |
| opt | Optimum |
| p | Pump |
| s | Source |
| max | maximum |
| sat | Saturation |
| th | Thermal |
| tur | Turbine |
| w | Water |

References

- [1] J. L. Pellegrino, N. Margolis, M. Miller, M. Justiniano. Energy Footprint Series: U.S. Manufacturing and Mining, Energetics, Incorporated, Columbia, Maryland, for the U.S. Department of Energy, Industrial Technology Programs, November 2003.
- [2] J. L. Pellegrino, N. Margolis, M. Miller, M. Justiniano, A. Thedki. Energy Use, Loss and Opportunities Analysis: U.S. Manufacturing and Mining. Energetics, Inc. and E3M, Inc. for the U.S. Department of Energy, Industrial Technologies Program 2004.
- [3] V. V. Viswanathan, R. W. Davies, J. D. Holbery. Opportunity Analysis for Recovering Energy from Industrial Waste Heat and Emissions, April 1st 2006.
- [4] I. BCS, "Waste Heat Recovery: Technology and Opportunities in U.S. Industry," March 2008.
- [5] Z. Wang, N. J. Zhou, J. Guo, X. Y. Wang, Fluid selection and parametric optimization of organic Rankine cycle using low temperature waste heat. *Energy* 40 (2012) 107-115
- [6] R. Scaccabarozzi, M. Tavano, C. M. Invernizzi, E. Martelli, Comparison of working fluids and cycle optimization for heat recovery ORCs from large internal combustion engines. *Energy* 158 (2018) 396- 416.
- [7] A.P. Weiß, T. Popp a, G. Zinn, M. Preißinger, D. Brüggeman. A micro-turbine-generator-construction-kit (MTG-c-kit) for small scale waste heat recovery ORC-Plants. *Energy* 181 (2019) 51 - 55.
- [8] J. Wang, Z. Yan, P. Zhao, Y. Dai. Off-design performance analysis of a solar- powered organic Rankine cycles. *Energy conversion and management* 80 (2014) 150-157.
- [9] S. Karellas, K. Braimakis. Energy–exergy analysis and economic investigation of a cogeneration and trigeneration ORC–VCC hybrid system utilizing biomass fuel and solar power *Energy Conversion and Management*. (In Press, Corrected Proof Available online 9 July 2015).
- [10] S. Wanga, Z. Fua. Thermodynamic and economic analysis of solar assisted CCHP-ORC system with DME as fuel. *Energy Conversion and Management* 186 (2019) 535–545.
- [11] S. M. Bina, S. Jalilinarabady, H. Fuju. Thermo-economic evaluation of various bottoming of optimum cycle for Sabalan power plant exhaust. *Geothermics* 70 (2017) 181-191.
- [12] J. Wang, P. Xu, T. Li, J. Zhu. Performance enhancement of organic Rankine cycle with two-stage evaporation using energy and exergy analyses, *Geothermics* 65 (2017) 126–134.
- [13] A.H. Mosaffaa, N. Hasani Mokarrama, L. Garousi Farshi. Thermo-economic analysis of combined different ORCs geothermal power plants and LNG cold energy. *Geothermics* 65 (2017) 113–125.
- [14] M. Imran, M. Usman, B-S. Park, Y. Yang. Comparative assessment of Organic Rankine Cycle

- integration for low temperature geothermal heat source applications. *Energy* 102 (2016) 473-490.
- [15] Agromayor R, Nord L.O. Fluid selection and thermodynamic optimization of organic Rankine cycles for waste heat recovery applications. *Energy procedia* 129 (2017) 527-534.
- [16] P J. Mago, LM. Chambrá, K. Srinivasan, Somayaji C. An examination of regenerative organic Rankine cycles using dry fluids. *Applied thermal Engineering* 28 (2008) 998-1007.
- [17] B. Saleh, G. Koglbauer, M. Wendland, J. Fischer. Working fluids for low-temperature organic Rankine cycle. *Energy* 32 (2017) 1210-1221.
- [18] W. Su, L. Zhao, S. Deng, Simulation working fluids design and cycle optimization for Organic Rankine cycle using group contribution model. *Applied energy* 202 (2017) 618-627.
- [19] E. Özah, A. Tozlu, A. Abuşoğlu, Thermo-economic multi-objective optimization of an organic Rankine cycle (ORC) adapted to an existing solid waste power plant, *Energy conversion and Management* 168 (2018), 308-319.
- [20] K. Thurairaja, A. Wijewardane, S. Jayasekaraa, C. Ranasinghe, Working Fluid Selection and Performance Evaluation of ORC. *Energy Procedia* 156 (2019) 244–248.
- [21] S. Quoilin, S. Declaye, B.F. Tchanche, V. Lamort, Thermo-economic optimization of waste heat recovery. *Applied Thermal Engineering* 31 (2011) 2885-2893.
- [22] J. Vivian, G. Manente, A. Lazzaretto, A general framework to select working fluid and configuration of ORCs for low to medium temperature heat sources. *Appl Energy* 156 (2015) 727-746.
- [23] J. Haervig, K. Sorensen, T.J. Condra, Guidelines for optimal selection of working fluid for an organic Rankine cycle in relation to waste heat recovery. *Energy* 96 (2016) 592-602.
- [24] Y-R. Li, M-T. Du, C-M. Wu, S-Y. Wu, C. Liu, 2014. Potential of organic Rankine cycle using zeotropic mixtures as working fluids for waste heat recovery. *Energy* 77 (2014) 509– 519.
- [25] J. Bao, L. Zhao, A review of working fluid and expander selection for organic Rankine cycle. *Renew Sustain Energy rev* 24 (2013) 325-342.
- [26] Milad Ashouri, Mohammad Hossein Ahmadi, Michel Feidt, Performance analysis of organic Rankine cycle integrated with a parabolic through solar collector. *World Sustainability Forum 2014 Conference Proceedings Paper*.
- [27] A.H. Mosaffa, N.H. Mokarram, L. GarousiFarshi, Thermo-economic analysis of combined different ORCs geothermal power plants and LNG cold energy. *Geothermics* 65 (2017) 113–125.
- [28] AC. McMahan, Design and optimization of organic Rankine cycle-solar thermal power plants. University of Wisconsin-Madison 2006.
- [29] F. Chouaibi, J. Belghaieb, N. Hajji, Waste Heat Recovery in a Sulfuric Acid Production Unit, in: F. Aloui, I. Dincer, *Energy for Better Environment and Improved Sustainability 1 Fundamentals*, Springer International Publishing A G, part of Springer Nature (2018) 931-942.
- [30] F. Vélez, J.J. Segovia, M.C. Martín, G. Antolin, F. Chejne, A. Quijano. Comparative study of working fluids for a Rankine cycle operating at low temperature. *Fuel processing Technology* 103 (2012) 71-77.
- [31] E. H. Wang, H. G. Zhang, B. Y. Fan, M. G. Ouyang, Y. Zhao, O. H. Mu. Study of working fluid selection of organic Rankine cycle (ORC) for engine waste heat recovery. *Energy* 36 (2011) 3406 – 3418.
- [32] S. Quoilin, Sustainable energy conversion through the use of Organic Rankine Cycles for waste heat recovery and solar applications. University of Liège; 2011 (<http://orbi.ulg.ac.be/handle/2268/96436>).
- [33] H. Chen, D.Y. Goswami, E.K. Stefanakos, A review of thermodynamic cycles and working fluids for the conversion of low-grade heat. *Renewable Sustainable Energy Rev* 14 (2010) 3059–3067. <http://dx.doi.org/10.1016/j.rser.2010.07.006>
- [34] WJ. Yang, CH. Kuo, O. Aydin, A hybrid power generation system: solar-driven Rankine engine-hydrogen storage. *Int J Energy Res* 25 (2001) 1107–1125. <http://dx.doi.org/10.1002/er.744>.
- [35] H. Chen, D.Y. Goswami, E.K. Stefanakos. A review of thermodynamic cycles and working fluids for the conversion of low-grade heat. *Renewable Sustainable Energy Rev* 14 (2010) 3059–3067. <http://dx.doi.org/10.1016/j.rser.2010.07.006>.
- [36] Ali Akbar Shayesteh, Omid Koohsheka, Amir Ghasemi, Mohammad Nematib, Hamid Mokhtari. Determination of the ORC-RO system optimum parameters based on 4E analysis; Water–Energy–Environment nexus. *Energy conversion and management* 183 (2019) 772 -790.
- [37] Xingchao Wanga, Edward K. Levya, Chun jian Pana, Carlos E. Romeroa, Arindam Banerjeeb, Carlos Rubio-Mayac, Lehua Pand. Working fluid selection for organic Rankine cycle power generation using hot produced supercritical CO₂ from a geothermal reservoir. *Applied Thermal Engineering* 149 (2019) 1287- 1304.
- [38] Nishith B. Desai, Santanu Bandyopadhyay; Thermo-economic analysis and selection of working fluid for solar organic Rankine cycle. *Applied Thermal engineering* 95 (2016) 471 – 481.
- [39] L. Afif , A. Elamari , N. Bouaziz. Energetic study and comparative analysis of two novel ORC cogeneration systems using gas ejectors. *Energy Procedia* 157 (2019) 1220–1229.
- [40] H. Zhang, X. Guan, Y. Ding, C. Liu, merger analysis of organic Rankine cycle (ORC) for waste heat power generation, *Journal of Cleaner Production* (2018).

- [41] O. Badr, S.D. Probert, P.W. O'Callaghan, Selecting a working fluid for a Rankine cycle engine, *Applied Energy* 21 (1985) 1–42.
- [42] S. Sadeghi, H. Saffari, N. Bahadormanesh. Optimization of a modified double-turbine Kalina cycle by using Artificial Bee Colony algorithm. *Applied Thermal Engineering* 91 (2015) 19-32.
- [43] S.Wang, Z. F. Thermodynamic and economic analysis of solar assisted CCHP – ORC system with DME as fuel. *Energy Conversion and Management*. 186 (2019) 535-545.
- [44] ArezuZeynalia, Ali Akbarib, Morteza Khalilian, Investigation of the performance of modified organic Rankine cycles (ORCs) and modified trilateral flash cycles (TFCs) assisted by a solar pond. *Solar energy* 182 (2019) 361 – 381.

Figures captions

Fig.1 Organic Rankine cycle and hot water loop.

Fig.2 Thermal efficiency as a function of condensation temperature for different fluids.

Fig.3 Thermal efficiency as a function of condensation pressure for different fluids.

Fig.4 Thermal efficiency as a function of evaporation temperature for different fluids.

Fig.5 Thermal efficiency and vapor fraction at the outlet of the turbine (x_2) as a function of the evaporation pressure for ammonia.

Fig.6 Thermal efficiency as a function of turbine efficiency for different fluids.

Fig.7 Thermal efficiency as a function of pump efficiency for different fluids.

Fig.8 Thermal efficiency as a function of the evaporation pressure for different fluids.

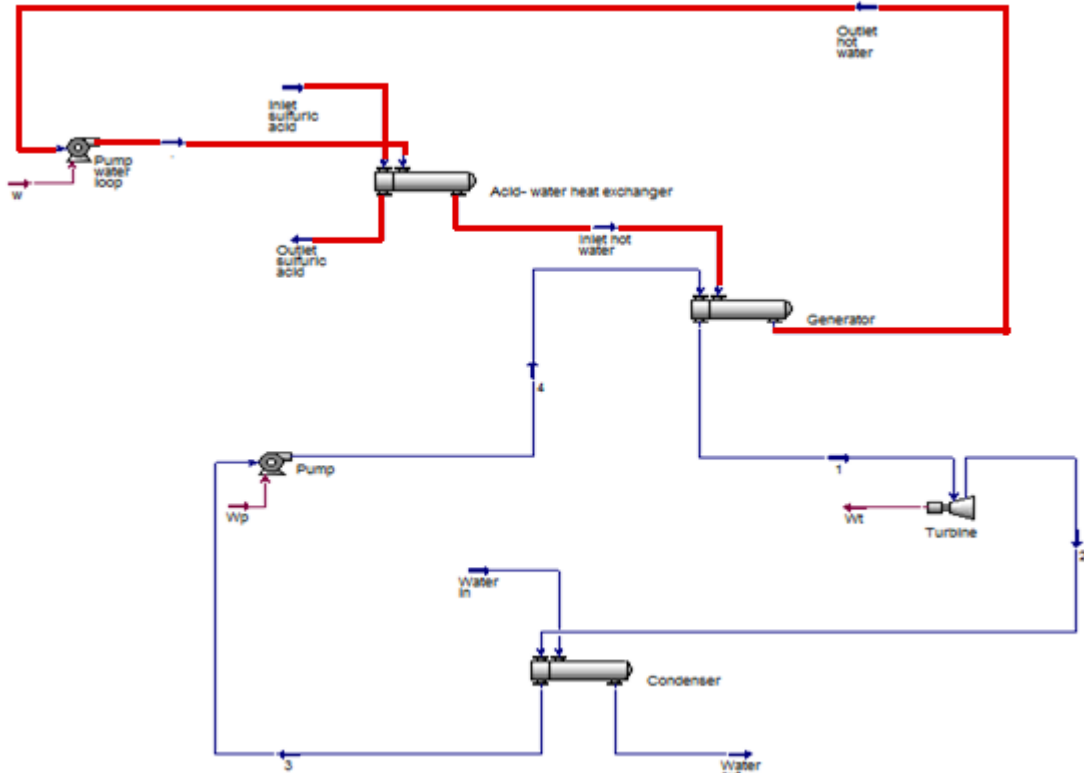


Fig. 1 Organic Rankine cycle and water loop.

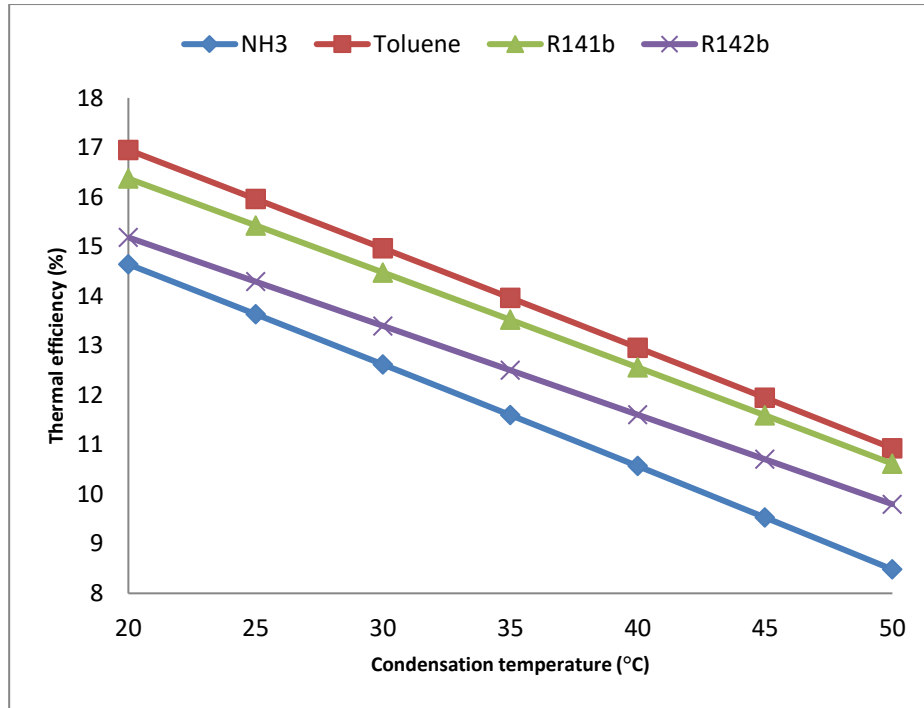


Fig.2 Thermal efficiency as a function of condensation temperature for different fluids.

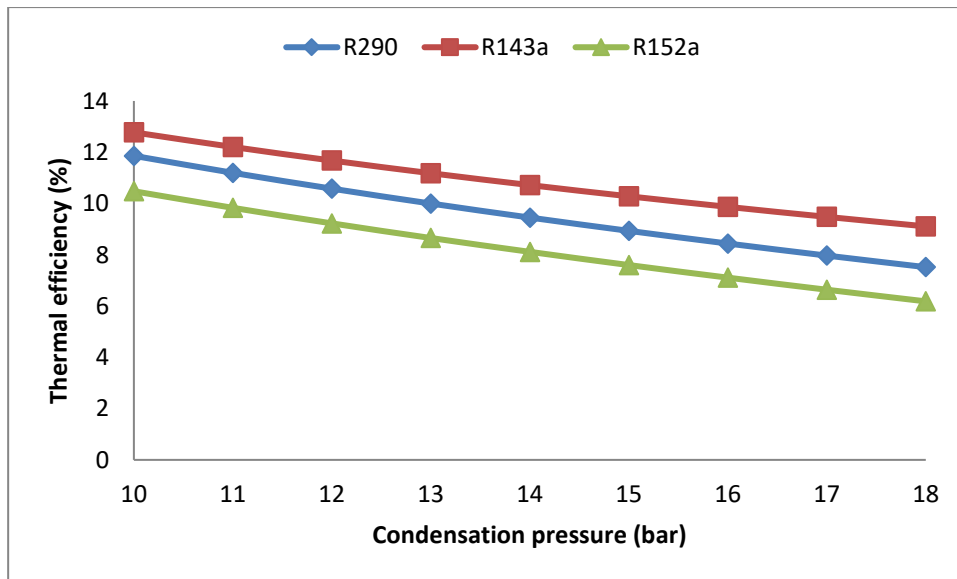


Fig.3 Thermal efficiency as a function of condensation pressure for different fluids.

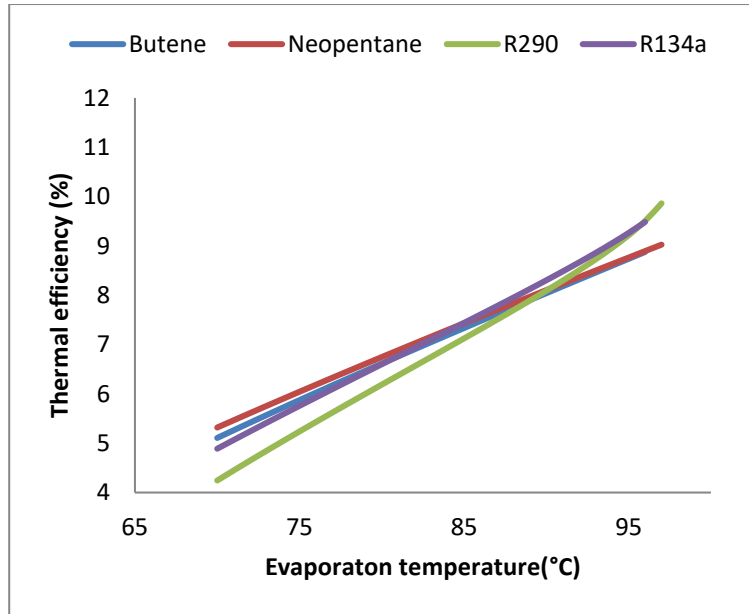


Fig.4 Thermal efficiency as a function of evaporation temperature for different fluids.

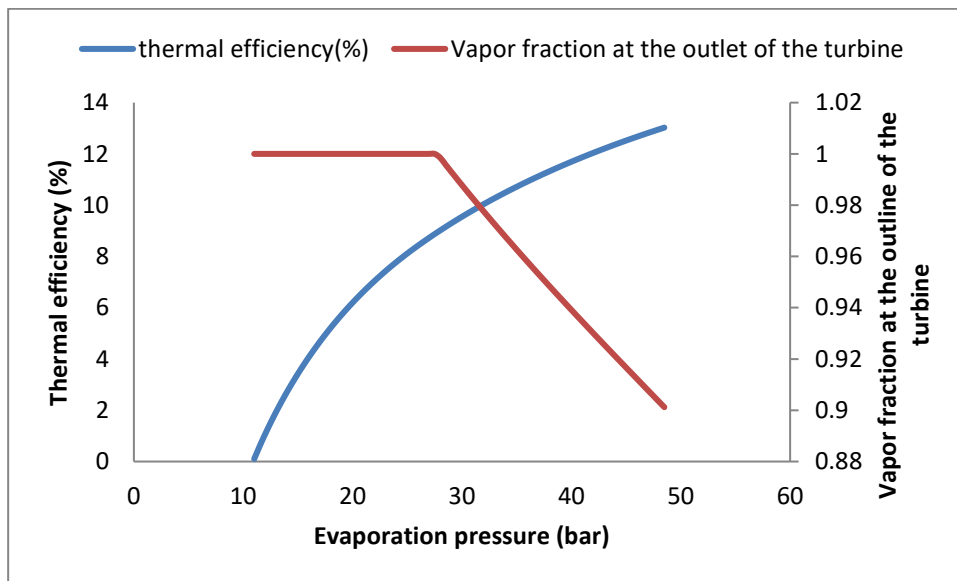


Fig.5 Thermal efficiency and vapor fraction at the outlet of the turbine (x_2) as a function of the evaporation pressure for ammonia.

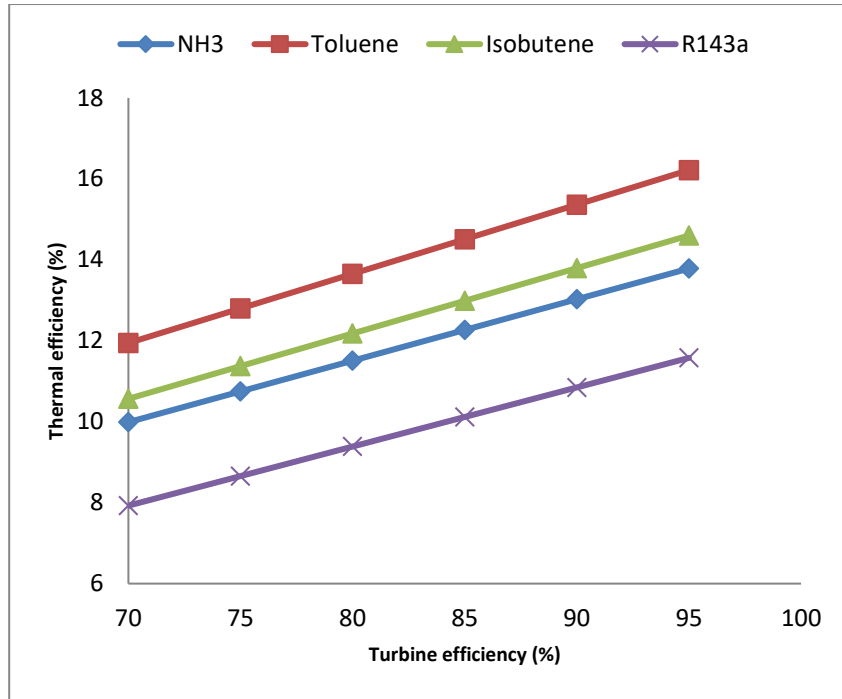


Fig.6 Thermal efficiency as a function of turbine efficiency for different fluids.

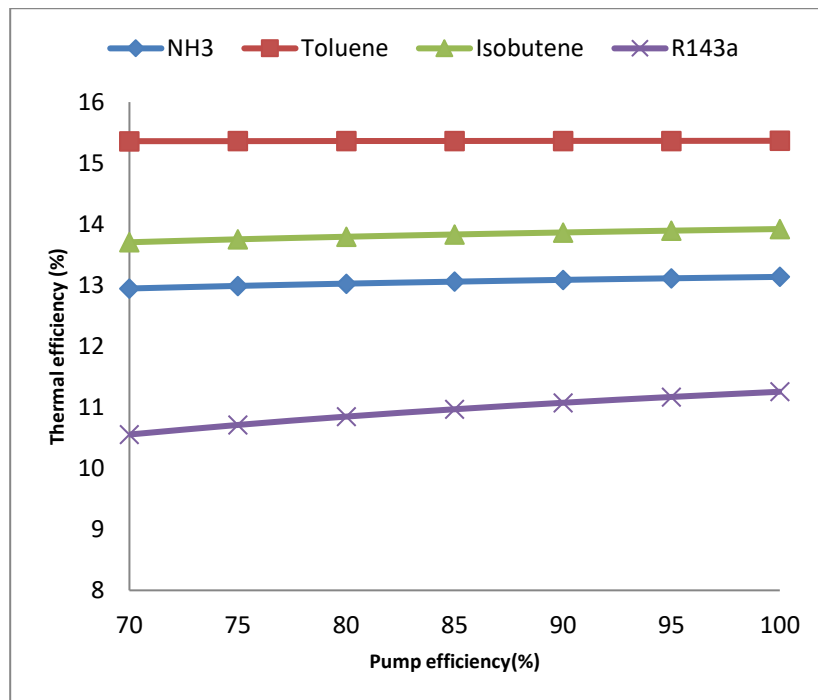
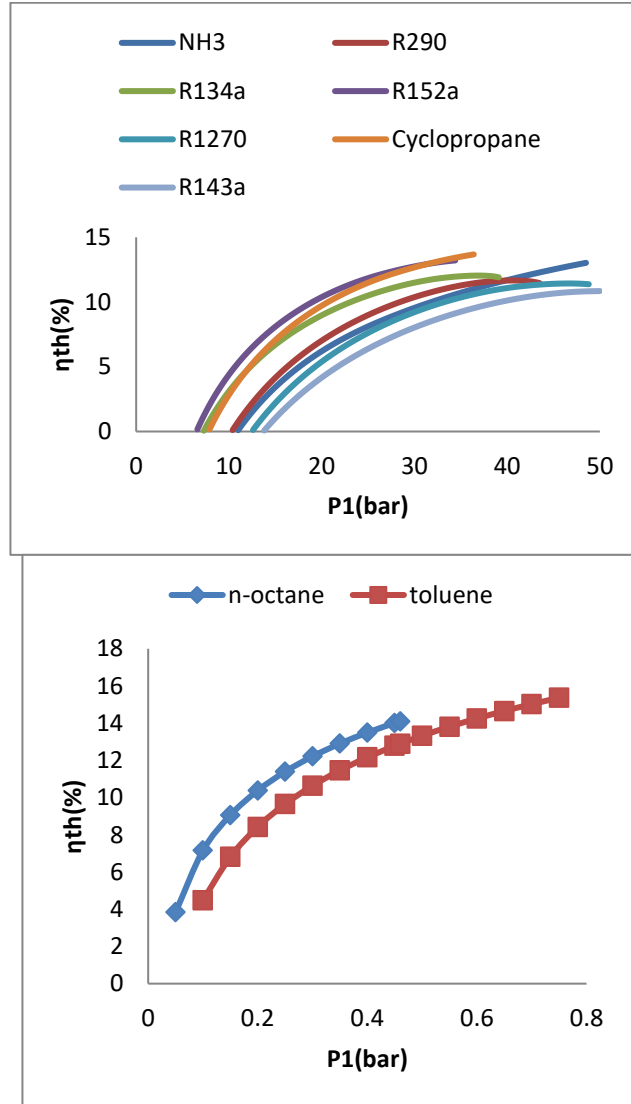


Fig.7 Thermal efficiency as a function of pump efficiency for different fluids.



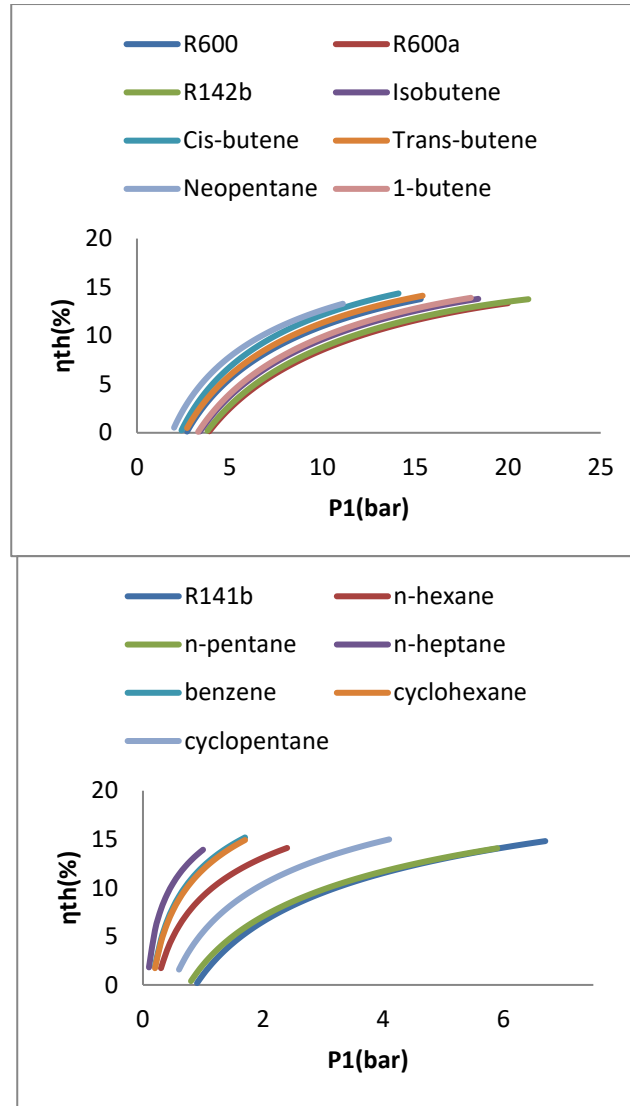


Fig.8 Thermal efficiency as a function of the evaporation pressure for different fluids.

Table 1 Properties of different working fluids studied in this work[6] [36- 38].

| Fluid | Slope | ρ (kg/ m ³) | Critic pressure (bar) | Critic temperature (°C) | Freezing poi (°C) | Boiling point (°C | Molecula Weigh (°C) | GWP | ODP | ASHRAE classification |
|------------------------------|----------|---------------------------------|-----------------------------|-------------------------------|----------------------|----------------------|------------------------|---------------|-------------|--------------------------|
| <i>NH3</i> | <i>W</i> | <i>616.1</i> | <i>112.80</i> | <i>132.4</i> | <i>-77.7</i> | <i>-33.33</i> | <i>17.03</i> | <i><1</i> | <i>0</i> | <i>B2</i> |
| <i>Benzene</i> | <i>D</i> | <i>882.2</i> | <i>49.24</i> | <i>288.9</i> | <i>5.5</i> | <i>80.1</i> | <i>114.2</i> | <i>-</i> | <i>-</i> | <i>-</i> |
| <i>1-Butene</i> | <i>D</i> | <i>593.8</i> | <i>40.23</i> | <i>145.47</i> | <i>-185.3</i> | <i>-6.47</i> | <i>56.11</i> | <i>-</i> | <i>-</i> | <i>-</i> |
| <i>cyclopentane</i> | <i>-</i> | <i>748.9</i> | <i>45.09</i> | <i>238.5</i> | <i>-94</i> | <i>49</i> | <i>70.14</i> | <i><11</i> | <i>0</i> | <i>-</i> |
| <i>Cyclohexane</i> | <i>D</i> | <i>781.8</i> | <i>40.53</i> | <i>280.1</i> | <i>-93.5</i> | <i>81</i> | <i>84.16</i> | <i>-</i> | <i>-</i> | <i>A1</i> |
| <i>Cyclopropane</i> | <i>-</i> | <i>1.8</i> | <i>54.90</i> | <i>124.65</i> | <i>-127</i> | <i>-32.9</i> | <i>42.08</i> | <i>-</i> | <i>0</i> | <i>-</i> |
| <i>Cis-butene</i> | <i>I</i> | <i>626</i> | <i>42.06</i> | <i>162.4</i> | <i>-</i> | <i>-</i> | <i>56.11</i> | <i>-</i> | <i>-</i> | <i>-</i> |
| <i>Isobutene</i> | <i>-</i> | <i>592.8</i> | <i>40.02</i> | <i>144.7</i> | <i>-140.03</i> | <i>-6.93</i> | <i>56.11</i> | <i>-</i> | <i>-</i> | <i>-</i> |
| <i>Neopentane</i> | <i>D</i> | <i>595.6</i> | <i>31.99</i> | <i>160.6</i> | <i>-16.1</i> | <i>10</i> | <i>72.15</i> | <i>-</i> | <i>-</i> | <i>-</i> |
| <i>n-hexane</i> | <i>D</i> | <i>655</i> | <i>29.90</i> | <i>234.45</i> | <i>-95.3</i> | <i>68.73</i> | <i>86.18</i> | <i>-</i> | <i>-</i> | <i>-</i> |
| <i>n-heptane</i> | <i>-</i> | <i>686.8</i> | <i>27.37</i> | <i>267</i> | <i>-91</i> | <i>98.42</i> | <i>100.2</i> | <i>-</i> | <i>-</i> | <i>-</i> |
| <i>n-pentane (R601)</i> | <i>D</i> | <i>692.7</i> | <i>33.75</i> | <i>196.5</i> | <i>-129.8</i> | <i>36.1</i> | <i>72.15</i> | <i>11</i> | <i>0</i> | <i>A3</i> |
| <i>n-octane</i> | <i>-</i> | <i>705.4</i> | <i>24.97</i> | <i>295.4</i> | <i>-56.8</i> | <i>125.67</i> | <i>114.2</i> | <i>-</i> | <i>-</i> | <i>-</i> |
| <i>Toluene</i> | <i>I</i> | <i>870</i> | <i>41.00</i> | <i>318.6</i> | <i>-95.2</i> | <i>110.6</i> | <i>92.14</i> | <i>2.7</i> | <i>0</i> | <i>-</i> |
| <i>Trans-butene</i> | <i>D</i> | <i>608.7</i> | <i>41.02</i> | <i>155.5</i> | <i>-</i> | <i>-</i> | <i>56.11</i> | <i>-</i> | <i>-</i> | <i>-</i> |
| <i>R1270: propylene</i> | <i>W</i> | <i>520.4</i> | <i>4.664</i> | <i>92.44</i> | <i>-185</i> | <i>-47.619</i> | <i>42,08</i> | <i>3</i> | <i>0</i> | <i>A3</i> |
| <i>R290: propanu</i> | <i>I</i> | <i>506.5</i> | <i>42.42</i> | <i>96.67</i> | <i>-189.9</i> | <i>96.7</i> | <i>44.1</i> | <i>20</i> | <i>0</i> | <i>A3</i> |
| <i>R134a</i> | <i>I</i> | <i>1242</i> | <i>40.56</i> | <i>101</i> | <i>-96.67</i> | <i>-26.11</i> | <i>102</i> | <i>1300</i> | <i>0</i> | <i>A1</i> |
| <i>R143a</i> | <i>W</i> | <i>1168</i> | <i>37.64</i> | <i>72.72</i> | <i>-111</i> | <i>-47.2</i> | <i>84.04</i> | <i>4300</i> | <i>0</i> | <i>A2</i> |
| <i>R152a</i> | <i>W</i> | <i>922.5</i> | <i>44.44</i> | <i>113.9</i> | <i>-117</i> | <i>-24</i> | <i>66.05</i> | <i>120</i> | <i>0</i> | <i>A2</i> |
| <i>R141b</i> | <i>I</i> | <i>1233</i> | <i>42.12</i> | <i>204.4</i> | <i>-103.5</i> | <i>32</i> | <i>116.9</i> | <i>700</i> | <i>0.11</i> | <i>A2</i> |
| <i>R142b</i> | <i>I</i> | <i>1124</i> | <i>41.20</i> | <i>137.1</i> | <i>-131.1</i> | <i>-10</i> | <i>100.5</i> | <i>2400</i> | <i>0.06</i> | <i>A2</i> |
| <i>R600a (Isobutane)</i> | <i>D</i> | <i>562.3</i> | <i>36.55</i> | <i>134.8</i> | <i>-145</i> | <i>135</i> | <i>58.12</i> | <i>20</i> | <i>0</i> | <i>A3</i> |
| <i>R600 (n-butane)</i> | <i>D</i> | <i>583.5</i> | <i>37.96</i> | <i>152</i> | <i>-138.3</i> | <i>0.5</i> | <i>58.12</i> | <i>-20</i> | <i>0</i> | <i>A3</i> |

Table 2 Operating parameters

| Parameter | Value |
|----------------------------------|-------|
| Temperature of the hot fluid | 110°C |
| Pressure of the hot fluid | 2 bar |
| Temperature of the cooling water | 23°C |
| Available power | 9 MW |
| Expander inlet temperature | 100°C |
| Turbine efficiency | 0.9 |
| Pump efficiency | 0.85 |
| Condensation temperature | 28°C |

Table 3 Maximum efficiency, mass flow rate and optimum evaporation pressure for each fluid for a condensation temperature of 28°C.

| Fluid | $\eta_{th, max}$ (%) | \dot{m}_n(kg/h) | P_{evop} (bar) | Power (kW) |
|---------------------|--|-------------------------------------|--|-------------------|
| <i>Benzene</i> | 15.44 | 64740 | 1.78 | 1389 |
| <i>Toluene</i> | 15.3 | 66110 | 0.74 | 1377 |
| <i>cyclopentane</i> | 15.1 | 66470 | 4.18 | 1359 |
| <i>Cyclohexane</i> | 15.02 | 67520 | 1.73 | 1352 |
| <i>R141b</i> | 14.86 | 119000 | 6.75 | 1337 |
| <i>Cis-butene</i> | 14.37 | 68800 | 14.16 | 1294 |
| <i>n-heptane</i> | 14.16 | 66470 | 1.05 | 1275 |
| <i>Trans-butene</i> | 14.12 | 68470 | 15.40 | 1270 |
| <i>n-hexane</i> | 14.11 | 66600 | 2.40 | 1270 |
| <i>n-octane</i> | 14.1 | 66680 | 0.46 | 1269 |
| <i>n-pentane</i> | 14.08 | 67220 | 5.90 | 1267 |
| <i>Isobutene</i> | 13.79 | 73560 | 18.40 | 1241 |
| <i>1-butene</i> | 13.77 | 73550 | 17.58 | 1239 |
| <i>R600</i> | 13.76 | 70830 | 15.26 | 1238 |
| <i>R142b</i> | 13.68 | 135300 | 20.78 | 1232 |
| <i>Cyclopropane</i> | 13.68 | 74800 | 36.45 | 1231 |
| <i>Neopentane</i> | 13.29 | 79290 | 11.17 | 1199 |
| <i>R600a</i> | 13.23 | 78520 | 19.56 | 1190 |
| <i>R152a</i> | 13.21 | 110800 | 34.45 | 1189 |
| <i>NH3</i> | 13.03 | 26150 | 48.50 | 1172 |
| <i>R134a</i> | 12.04 | 163500 | 36.30 | 1083 |
| <i>R290:propane</i> | 11.66 | 86740 | 39.80 | 1049 |
| <i>R1270</i> | 11.43 | 91700 | 46.60 | 1029 |
| <i>R143a</i> | 10.85 | 181800 | 50.00 | 976.2 |

Table 4 Maximum efficiency, Mass flow rate and optimum evaporation pressure for each fluid for a condensation temperature of 40 ° C.

| Fluid | $\eta_{th, max}(\%)$ | $\dot{m}_f(\text{kg/h})$ | P_{evop} (kPa) | Power (kW) |
|----------------------|--|--|--|-------------------|
| <i>Benzene</i> | 13.02 | 67260 | 1.78 | 1172 |
| <i>Toluene</i> | 12.92 | 68800 | 0.74 | 1160 |
| <i>Cyclopentane</i> | 12.74 | 69460 | 4.18 | 1147 |
| <i>Cyclohexane</i> | 12.67 | 70600 | 1.73 | 1141 |
| <i>R141b</i> | 12.56 | 125100 | 6.75 | 1130 |
| <i>Cis-butene</i> | 12.15 | 72910 | 14.16 | 1093 |
| <i>n-heptane</i> | 12 | 70530 | 1.05 | 1080 |
| <i>Trans-butene</i> | 11.94 | 72900 | 15.40 | 1074 |
| <i>n-hexane</i> | 11.94 | 70530 | 2.40 | 1075 |
| <i>n-octane</i> | 11.94 | 70440 | 0.46 | 1075 |
| <i>n-pentane</i> | 11.92 | 71350 | 5.90 | 1073 |
| <i>Isobutene</i> | 11.66 | 78750 | 18.40 | 1049 |
| <i>R600</i> | 11.63 | 75760 | 15.26 | 1047 |
| <i>1-Butene</i> | 11.59 | 78550 | 17.58 | 1043 |
| <i>R142b</i> | 11.52 | 144900 | 20.78 | 1037 |
| <i>Cyclopropane</i> | 11.51 | 79990 | 36.40 | 1036 |
| <i>Neopentane</i> | 11.31 | 85100 | 11.17 | 1018 |
| <i>R600a</i> | 11.14 | 84600 | 19.56 | 1002 |
| <i>R152a</i> | 11.14 | 120100 | 34.45 | 1003 |
| <i>NH3</i> | 11.07 | 27870 | 52.00 | 996.5 |
| <i>R1270</i> | 10.36 | 102600 | 47.20 | 843.2 |
| <i>R134a</i> | 10.02 | 182800 | 37.00 | 901.4 |
| <i>R290: propane</i> | 9.61 | 98160 | 41.00 | 865.5 |
| <i>R143a</i> | 8.99 | 220000 | 53.10 | 809 |

Table 5 Maximum efficiency, Mass flow rate and optimum evaporation pressure for each fluid for a condensation temperature of 50 ° C.

| Fluid | $\eta_{th,max}(\%)$ | $\dot{m}_f(\text{kg/h})$ | P_{evop} (kPa) | Power (kW) |
|---------------------|---------------------|--------------------------|------------------|--------------|
| <i>Benzene</i> | 10.98 | 69580 | 1.78 | 987.8 |
| <i>Toluene</i> | 10.91 | 71300 | 0.74 | 976.7 |
| <i>Cyclopentane</i> | 10.75 | 72280 | 4.18 | 967.5 |
| <i>Cyclohexane</i> | 10.7 | 73500 | 1.73 | 963 |
| <i>R141b</i> | 10.62 | 130800 | 6.75 | 955.5 |
| <i>Cis-butene</i> | 10.27 | 76860 | 14.16 | 924 |
| <i>n-heptane</i> | 10.18 | 74140 | 1.05 | 916 |
| <i>n-octane</i> | 10.12 | 74000 | 0.46 | 911 |
| <i>n-Hexane</i> | 10.11 | 74220 | 2.40 | 910 |
| <i>n-pentane</i> | 10.11 | 75310 | 5.90 | 910 |
| <i>Trans-butene</i> | 10.1 | 77210 | 15.40 | 908.8 |
| <i>Isobutene</i> | 9.86 | 83850 | 18.40 | 887.6 |
| <i>R600</i> | 9.84 | 80590 | 15.26 | 885.8 |
| <i>1-Butene</i> | 9.76 | 83450 | 17.58 | 878.6 |
| <i>R142b</i> | 9.7 | 154300 | 20.78 | 873 |
| <i>Cyclopropane</i> | 9.69 | 85240 | 36.40 | 872 |
| <i>Neopentane</i> | 9.6 | 90840 | 11.17 | 864 |
| <i>R152a</i> | 9.4 | 129600 | 34.45 | 846 |
| <i>R600a</i> | 9.37 | 90690 | 19.56 | 845 |
| <i>NH3</i> | 9.32 | 39450 | 54.00 | 839 |
| <i>R134a</i> | 8.35 | 12530 | 37.90 | 110 |
| <i>R290:propane</i> | 7.93 | 110100 | 41.60 | 714 |
| <i>R1270</i> | 7.67 | 115200 | 47.80 | 690 |
| <i>R143a</i> | 7.466 | 247700 | 51.30 | 672 |

Table 6 Comparison between results given by HYSYS and EES for a condensation temperature equal to 28°C.

| Fluids | $\eta_{th, max}(\%)$ | | Relative difference (%) |
|--------------------------|----------------------|-------|-------------------------|
| | HYSYS | EES | |
| <i>Benzene</i> | 15.44 | 15.35 | 0.58 |
| <i>Toluene</i> | 15.3 | 15.31 | 0.063 |
| <i>Cyclohexane</i> | 15.02 | 14.89 | 0.86 |
| <i>R141b</i> | 14.86 | 14.68 | 1.21 |
| <i>n-heptane</i> | 14.16 | 14.12 | 0.28 |
| <i>n-hexane</i> | 14.11 | 14.14 | 0.21 |
| <i>n-octane</i> | 14.1 | 14.13 | 0.21 |
| <i>n-pentane</i> | 14.08 | 14.03 | 0.35 |
| <i>Isobutene</i> | 13.79 | 13.91 | 0.87 |
| <i>1-butene</i> | 13.77 | 13.7 | 0.5 |
| <i>R600</i> | 13.76 | 13.86 | 0.72 |
| <i>R142b</i> | 13.68 | 13.9 | 1.67 |
| <i>Neopentane</i> | 13.29 | 13.37 | 0.6 |
| <i>R600a</i> | 13.23 | 13.14 | 0.68 |
| <i>R152a</i> | 13.21 | 13.2 | 0.075 |
| <i>NH3</i> | 13.03 | 13.08 | 0.38 |
| <i>R134a</i> | 12.04 | 12.26 | 1.82 |
| <i>R290:propane</i> | 11.66 | 12.01 | 3 |
| <i>R1270 (propylene)</i> | 11.43 | 11.82 | 3.41 |
| <i>R143a</i> | 10.85 | 10.72 | 1.19 |

Table 7 Comparison between results given by HYSYS and EES for a condensation temperature equal to 40°C.

| Fluids | $\eta_{th, max}(\%)$ | | Relative difference (%) |
|----------------------|----------------------|-------|-------------------------|
| | HYSYS | EES | |
| <i>Benzene</i> | 13.02 | 12.71 | 2.38 |
| <i>Toluene</i> | 12.92 | 12.93 | 0.077 |
| <i>Cyclohexane</i> | 12.67 | 12.56 | 0.86 |
| <i>R141b</i> | 12.56 | 12.42 | 1.11 |
| <i>n-heptane</i> | 12 | 11.97 | 0.25 |
| <i>n-hexane</i> | 11.94 | 12.02 | 0.67 |
| <i>n-octane</i> | 11.94 | 11.96 | 0.16 |
| <i>n-pentane</i> | 11.92 | 11.9 | 0.16 |
| <i>Isobutene</i> | 11.66 | 11.84 | 1.54 |
| <i>R600</i> | 11.63 | 11.74 | 0.94 |
| <i>1-Butene</i> | 11.59 | 11.56 | 0.25 |
| <i>R142b</i> | 11.52 | 11.76 | 2.08 |
| <i>Neopentane</i> | 11.31 | 11.76 | 3.97 |
| <i>R600a</i> | 11.14 | 11.13 | 0.18 |
| <i>R152a</i> | 11.14 | 11.12 | 0.17 |
| <i>NH3</i> | 11.07 | 11.12 | 0.45 |
| <i>R1270</i> | 10.36 | 9.88 | 4.63 |
| <i>R134a</i> | 10.02 | 10.24 | 2.19 |
| <i>R290: propane</i> | 9.61 | 9.975 | 3.79 |
| <i>R143a</i> | 8.99 | 8.656 | 3.7 |

Table 8 Comparison between results given by HYSYS and EES for a condensation temperature equal to 50°C.

| Fluids | $\eta_{th, max}(\%)$ | | Relative difference (%) |
|---------------------|----------------------|--------------|-------------------------|
| | HYSYS | EES | |
| <i>Benzene</i> | <i>10.98</i> | <i>10.72</i> | <i>2.36</i> |
| <i>Toluene</i> | <i>10.91</i> | <i>10.92</i> | <i>0.091</i> |
| <i>Cyclohexane</i> | <i>10.7</i> | <i>10.6</i> | <i>0.93</i> |
| <i>R141b</i> | <i>10.62</i> | <i>10.5</i> | <i>1.129</i> |
| <i>n-heptane</i> | <i>10.18</i> | <i>10.15</i> | <i>0.29</i> |
| <i>n-octane</i> | <i>10.12</i> | <i>10.13</i> | <i>0.09</i> |
| <i>n-Hexane</i> | <i>10.11</i> | <i>10.21</i> | <i>0.98</i> |
| <i>n-pentane</i> | <i>10.11</i> | <i>10.1</i> | <i>0.09</i> |
| <i>Isobutene</i> | <i>9.86</i> | <i>10.08</i> | <i>2.23</i> |
| <i>R600</i> | <i>9.84</i> | <i>9.948</i> | <i>1.09</i> |
| <i>1-Butene</i> | <i>9.76</i> | <i>9.783</i> | <i>2.45</i> |
| <i>R142b</i> | <i>9.7</i> | <i>9.938</i> | <i>2.45</i> |
| <i>Neopentane</i> | <i>9.6</i> | <i>9.654</i> | <i>0.56</i> |
| <i>R152a</i> | <i>9.4</i> | <i>9.372</i> | <i>0.29</i> |
| <i>R600a</i> | <i>9.37</i> | <i>9.427</i> | <i>0.6</i> |
| <i>NH3</i> | <i>9.32</i> | <i>9.362</i> | <i>0.4</i> |
| <i>R134a</i> | <i>8.35</i> | <i>8.568</i> | <i>2.61</i> |
| <i>R290:propane</i> | <i>7.93</i> | <i>8.274</i> | <i>4.33</i> |
| <i>R1270</i> | <i>7.67</i> | <i>8.027</i> | <i>4.65</i> |

Table 9 Input parameters values used in literature [31] for R141b.

| Parameter | Value |
|--|--------|
| Working fluid | R141b |
| Temperature of waste heat source (K) | 600 |
| Net power output (kW) | 10 |
| Condensation temperature (K) | 300 |
| Isentropic efficiency of the turbine (%) | 55 |
| Isentropic efficiency of the pump (%) | 80 |
| Evaporation temperature (K) | 420.12 |
| Evaporation pressure (bar) | 17.281 |

Table 10 Model comparison with published literature [31] for R141b.

| Simulation results | Thermal efficiency (%) | Produced power (kW) |
|--------------------------------|-------------------------------|----------------------------|
| This paper | 9.3 | 10.3 |
| Published literature | 9.28 | 10.0 |
| Relative difference (%) | 0.21 | 0.29 |